SERDP

EXECUTIVE SUMMARY

Thermal-Enhanced Photochemical and Alkaline Destruction of PFAS in Sorbent Regenerants and Membrane Concentrates

Jinyong Liu
University of California, Riverside

January 2025

SERDP Project ER21-1117

SERDP EXECUTIVE SUMMARY

Project: ER21-1117

TABLE OF CONTENTS

LIST OF FIGURES

LIST OF TABLES

ACRONYMS AND ABBREVIATIONS

deF%	defluorination percentage
e_{aq}^-	hydrated electrons
ESTCP	Environmental Security Technology Certification Program
FTCA	fluorotelomer carbonic acid
PFAS	per- and polyfluoroalkyl substances
PFBS	perfluorobutane sulfonic acid
PFCA	perfluoro carboxylic acid
PFHxS	perfluorohexane sulfonic acid
PFOA	perfluorooctanoic acid
PFOS	perfluorooctane sulfonic acid
PFSA	perfluoro sulfonic acid
PI	principal investigator
SERDP	Strategic Environmental Research and Development Program
UV	ultra-violet

ACKNOWLEDGEMENT

This report represents the results and conclusions from Dr. Jinyu Gao (Tasks 1 and 3), and Dr. Dandan Rao (Task 2). Early-stage development for preliminary results was contributed by Dr. Zekun Liu under the support by Strategic Environmental Research and Development Program (SERDP) ER18-1289. The project team thanks Dr. Andrea Leeson and the support staff from the SERDP office for their help and guidance.

1.0 INTRODUCTION

Among the recently developed per- and polyfluoroalkyl substances (PFAS) degradation technologies that could work at ambient temperature and pressure, the ultra-violet (UV)/sulfite system stood out for its excellent performance and low consumption of chemicals and energy. UV/sulfite generated hydrated electrons (e_{aq}^-) that could effectively cleave C–F bonds in PFAS. Previously, the principal investigator's (PI) lab and many other labs maintained the temperature of UV/sulfite treatment at 20°C or lower using a cooling jacket to simulate typical ambient conditions in natural waters. In the absence of the cooling jacket, however, the heat generated by the UV lamp could raise the water temperature, potentially expediting the reaction and improving the defluorination percentage (deF%). When this project was proposed in early 2020, the treatment performance and underlying mechanism regarding temperature effects on PFAS degradation under the UV/sulfite system were unknown.

The project team also anticipated that adjusting the number of UV lamps would expedite PFAS defluorination not only because of the irradiation intensity but also due to the temperature change by heat dissipation from UV lamps. When the project was proposed, it was unclear whether adding more UV lamps and removing the cooling system could help cleave additional C–F bonds toward a higher overall deF%. Adding more UV lamps entailed higher energy consumption, and it was unclear whether this approach could proportionally enhance the rate or extent of PFAS defluorination.

During early explorations, the PI's lab also observed spontaneous defluorination from specific H-containing polyfluorinated structures at pH 12. The defluorination became faster in the presence of elevated temperature (below the water boiling point of 100 °C) and alkaline conditions (pH 9–14, without UV/sulfite treatment). Under the same conditions, the corresponding fully fluorinated structures showed no reactivity. This phenomenon prompted the project team to consider that H atoms in polyfluorinated structures might initiate new defluorination mechanisms independent of redox processes and C−F bond dissociation energies.

With the knowledge gaps presented above, for this project, the project team primarily aimed to elucidate the reaction mechanisms underlying the thermal enhancement of PFAS degradation, with (Task 1) or without (Task 2) UV/sulfite treatment, and to further optimize energy efficiency by determining the optimal reaction temperature and the number of UV lamps (Task 3).

2.0 OBJECTIVES

The overall objectives of this limited-scope project were to obtain a comprehensive understanding and determine key parameters for the thermal-enhanced reductive and alkaline destruction of PFAS. The direct technical goal was to use a limited amount of thermal energy (i.e., heating the water up to 90°C) to enhance the treatment effectiveness and energy efficiency for PFAS degradation. The outcomes validated the "thermal-enhanced" treatment strategy and will benefit the management of PFAS-enriched waste streams in practical demonstration projects.

Three specific objectives were:

(i) Achieve deep or near-complete defluorination from a majority of PFAS structures by the thermal-enhanced single-step UV/sulfite treatment; if not successful, elucidate the effect of temperature and the reaction mechanisms.
(ii) Achieve rapid decay and deep defluorination of recalcitrant PFAS structures such as short-chain sulfonic acids and fluorotelomers by thermal-enhanced photochemical and alkaline treatment; if not successful, elucidate the structure-reactivity relationship and the reaction mechanism.
(iii) Minimize the consumption of both electricity and chemicals through the thermal-enhanced treatment strategy.

3.0 TECHNICAL APPROACH

Preparation of stock solutions of PFAS and reaction chemicals. The PFAS were purchased in bulk quantities (0.1–5 g) and used as received. Individual PFASs were dissolved in deionized water as 10 mM stock solutions, and 10 mM NaOH was added to facilitate the dissolution of long-chain structures in water and avoid the volatilization of short-chain structures. The PFAS stock solutions were stored on the benchtop at room temperature (around 20°C). Sodium sulfite (Na_2SO_3), potassium iodide (KI), sodium bicarbonate ($NaHCO_3$), and sodium hydroxide (NaOH) were purchased from Fisher Chemical.

Photochemical reactor design and setup. The photoreactor was customized from a 2 L beaker wrapped with aluminum foil and covered by a plastic cap with parafilm sealing. A low-pressure mercury lamp (GPH212T5L, 254 nm, 10 Watt) enveloped in a quartz sleeve was placed in the center of the beaker. The beaker was loaded with 2 L of deionized water and placed on a magnetic stirring hotplate (Thermo Scientific Cimarec+) with temperature-controlled heating to the designated temperature between 40 and 90°C (±2°C variance). The probe thermometer was inserted into the solution through a self-healing rubber injection port on the plastic cap. Upon reaching the desired temperature, 25 μM of PFAS, 10 mM of Na_2SO_3, 5 mM of $NaHCO_3$, and 4 mL of 10 N NaOH (for pH adjustment to 12) were added to the water through the sampling port on the cap. The UV light was then turned on to initiate PFAS degradation. For the reaction started at 20°C, the water was slowly heated by the UV lamp (no hotplate heating or water bath cooling) to 36°C within the first 4 h and then maintained at 36°C by the balance between generation and dissipation of heat. Aliquots of solution (6 mL each) were taken at regular intervals using syringes and stored for further analysis.

PFAS degradation and transformation product analysis with liquid chromatography-high-resolution mass spectrometry. An ultra-high-performance liquid chromatography equipped with a high-resolution quadrupole orbitrap mass spectrometer (UHPLC−HRMS/MS) (Q Exactive, Thermo Fisher Scientific) was used to analysis PFAS parent compounds and their transformation products. For UHPLC separation, the mobile phase used (A) 10 mM ammonium acetate in Milli-Q water and (B) 10 mM ammonium acetate in HPLC-grade methanol. A 2-μL sample was loaded onto a Hypersil GOLD column (particle size 1.9 μm, 100×2.1 mm, Thermo Fisher Scientific) and eluted at a flow rate of 300 μL/min. Gradient: 95% A for 0−1 min, 95%−5% A for 1−6 min, 5% A for 6−8 min, and 95% A for 8−10 min. The parent compounds and TPs were detected in full scan negative ionization mode on HRMS at a resolution of 70,000 at m/z 200 and a scan range of m/z 50−750. Data analysis used Freestyle 1.6 and TraceFinder 4.1 EFS (Thermo Fisher Scientific).

Measurement of fluoride ion release. The released fluoride ion (F^-) was measured by an ion-selective electrode and validated by ion chromatography (IC). The defluorination percentage (deF%) represents the ratio between the released F^- and the total F in the original PFAS.

Quantification of short-chain perfluoro carboxylic acids (PFCA) and sulfite with ion chromatography. The concentrations of short-chain organic anions and sulfite were analyzed by a Dionex ICS-5000 ion chromatography (IC) system equipped with a conductivity detector and suppressor (AERS 4 mm) and a Dionex ICS-6000 EG eluent generator using an EGC 500 KOH cartridge. The separation of the anions used an IonPac AS11-HC analytical column (4 × 250 mm) in line with an AG11-HC guard column (4 × 50 mm). Specific methods for each analyte are below:

- TFA: Isocratic, 1.0 mL min^{-1}, 10 mM KOH, 30°C, 30 minutes;
- PFPrA: Isocratic, 1.5 mL min^{-1} , 20 mM KOH, 30°C, 20 minutes;
- Sulfite: Isocratic, 1.0 mL min^{-1}, 20 mM KOH, 30°C, 20 minutes.

4.0 RESULTS AND DISCUSSION

Throughout this project, the project team collected a comprehensive set of performance data and advanced the engineering aspects of UV/sulfite technology toward field demonstration operations (Environmental Security Technology Certification Program (ESTCP) ER21-5152). The project team elucidated detailed mechanisms for thermal-enhanced PFAS degradation regarding: (1) the optimal temperature at 50°C rather than 90°C, (2) the key photochemical parameters that determined the reaction rate, and (3) the role of hydroxide and structure-reactivity relationship in non-photochemical alkaline defluorination. The findings provided novel perceptions of thermal energy effects in the photochemical system.

Thermal-enhanced UV/sulfite defluorination. The **first highlight of this project** was the systematic investigation of the effect of temperature on PFAS degradation under UV/sulfite treatment. The highest rates of PFAS decay and defluorination were achieved at 50°C (Figure ES-1 and Table ES-1). For the three major PFAS structure families (PFCAs, perfluoro sulfonic acids (PFSA), and fluorotelomer carbonic acids (FTCA)), the decay rates increased by 21–85% when the solution temperature was raised from 20 to 50°C. For the recalcitrant structures that could not be effectively degraded by UV/sulfite treatment (e.g., n=4 perfluorobutane sulfonic acid (PFBS) and 4:3 FTCA), the percentage of decay was also improved by 9–19% after 24 h. The deF% also increased by 3–22% (particularly significant for recalcitrant PFAS structures). The transformation product analysis suggested that the reaction at 50°C also allowed the cleavage of relatively strong C–F bonds.

In contrast, further raising the temperature to 90°C resulted in adverse effects. Compared to 20°C, the rates of PFAS decay decreased by 41–66% at 90°C. The percentages of decay and defluorination were similar to those at 20°C, but the rates were slower. Photochemical measurements suggested that the elevated temperature lowered the quantum yield of e_{aq}^-. The competition between accelerated elemental reaction steps versus decreased quantum yield of e_{aq}^- resulted in the maximum rate for the overall reaction at 50°C. Further increasing the temperature to up to 90°C resulted in a gradual slowing down of the overall reaction.

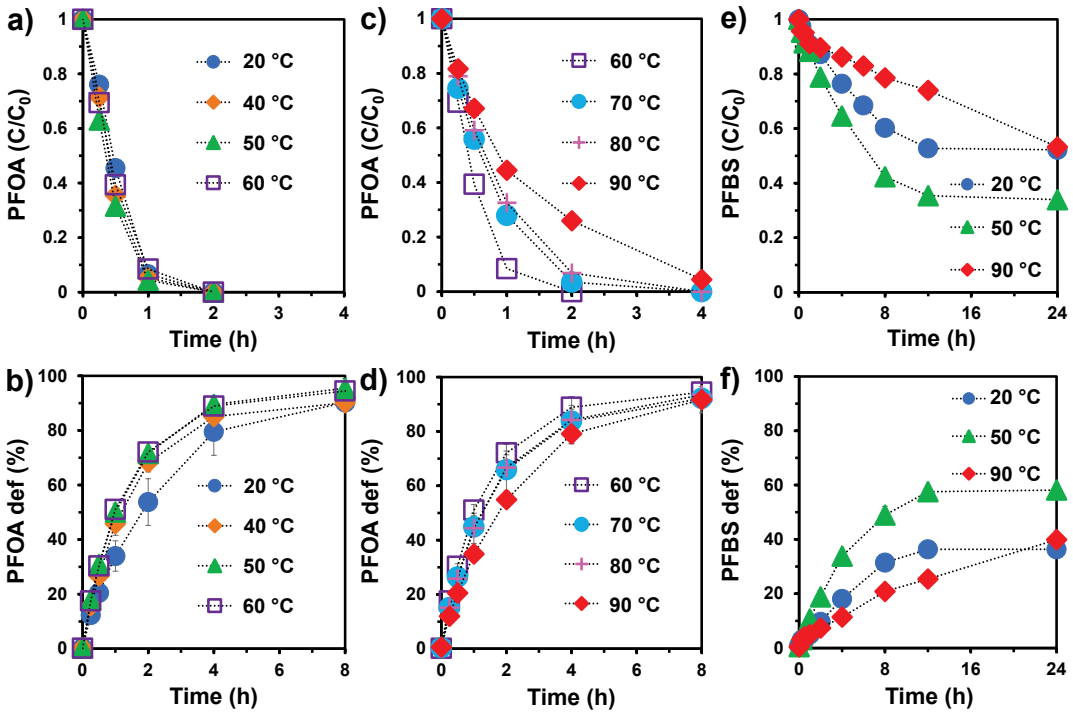

Figure ES-1. Profiles for (a, c, and e) Parent Compound Decay and (b, d, and f) Defluorination of Perfluorooctanoic Acid (PFOA) and PFBS at Various Temperatures.

Reaction conditions: individual PFAS (25 μM), Na_2SO_3 (10 mM), $NaHCO_3$ (5 mM), pH 12.0, and 254 nm irradiation (10 W lamp for 2 L solution).

Table ES-1. Defluorination Ratio and Rate Constant of PFAS by UV/Sulfite Treatment at 20, 50, and 90°C.[a]

PFCA ($C_nF_{2n+1}COO^-$)	def% after 8 h			decay rate in h^{-1} (decay% after 8 h)		
	20 °C	50 °C	90 °C	20 °C	50 °C	90 °C
n = 1 TFA	99 ± 2.0	99 ± 0.5	96 ± 2.5	2.15 (> 99)	2.60 (> 99)	0.72 (> 99)
n = 2 PFPrA	76 ± 5.7	89 ± 1.5	89 ± 4.2	2.01 (> 99)	2.72 (> 99)	0.81 (> 99)
n = 3 PFBA	92 ± 2.8	95 ± 0.4	94 ± 0.9	1.73 (> 99)	2.92 (> 99)	0.82 (> 99)
n = 4 PFPeA	85 ± 3.0	91 ± 2.5	88 ± 2.5	1.70 (> 99)	2.75 (> 99)	0.83 (> 99)
n = 5 PFHxA	86 ± 0.5	90 ± 0.4	87 ± 4.5	1.50 (> 99)	2.74 (> 99)	0.77 (> 99)
n = 6 PFHpA	83 ± 2.7	86 ± 1.8	85 ± 4.9	1.28 (> 99)	2.19 (> 99)	0.62 (> 99)
n = 7 PFOA	90 ± 0.6	95 ± 3.6	92 ± 4.9	1.58 (> 99)	2.31 (> 99)	0.67 (> 99)
PFSA ($C_nF_{2n+1}SO_3^-$)	**def% after 24 h**			**decay rate in h^{-1} (decay% after 24 h)**		
	20 °C	**50 °C**	**90 °C**	**20 °C**	**50 °C**	**90 °C**
n = 4 PFBS	36 ± 0.5	58 ± 0.2	40 ± 3.5	0.05 (47)	0.09 (66)	0.02 (48)
n = 6 PFHxS	74 ± 2.7	86 ± 2.2	79 ± 0.8	0.27 (> 99)	0.50 (> 99)	0.10 (96)
n = 8 PFOS	88 ± 3.8	89 ± 2.9	87 ± 3.7	0.75 (> 99)	1.22 (> 99)	0.41 (> 99)
FTCA ($C_nF_{2n+1}CH_2CH_2COO^-$)	**def% after 24 h**			**decay rate in h^{-1} (decay% after 24 h)**		
	20 °C	**50 °C**	**90 °C**	**20 °C**	**50 °C**	**90 °C**
n = 4 FTCA	12 ± 0.4	22 ± 1.8	9 ± 0.5	< 0.01 (12)	< 0.01 (21)	< 0.01 (8)
n = 6 FTCA	68 ± 4.1	86 ± 4.5	72 ± 5.7	0.19 (89)	0.35 (> 99)	0.07 (85)
n = 8 FTCA	78 ± 4.4	86 ± 2.6	86 ± 4.0	0.58 (> 99)	0.79 (> 99)	0.34 (99)

[a]Reaction conditions: individual PFAS (25 μM), Na_2SO_3 (10 mM), $NaHCO_3$ (5 mM), pH 12.0, and 254 nm irradiation (10 W low-pressure Hg lamp for 2 L solution).

The addition of iodide for reaction acceleration also benefited from the elevated temperature to 50°C (Figure ES-2). However, iodide addition did not alter the PFAS degradation mechanism, so the maximum deF% by UV/sulfite+iodide was the same as by UV/sulfite. The positive effects from both iodide addition and heating to 50°C could synergistically achieve significantly enhanced defluorination performance.

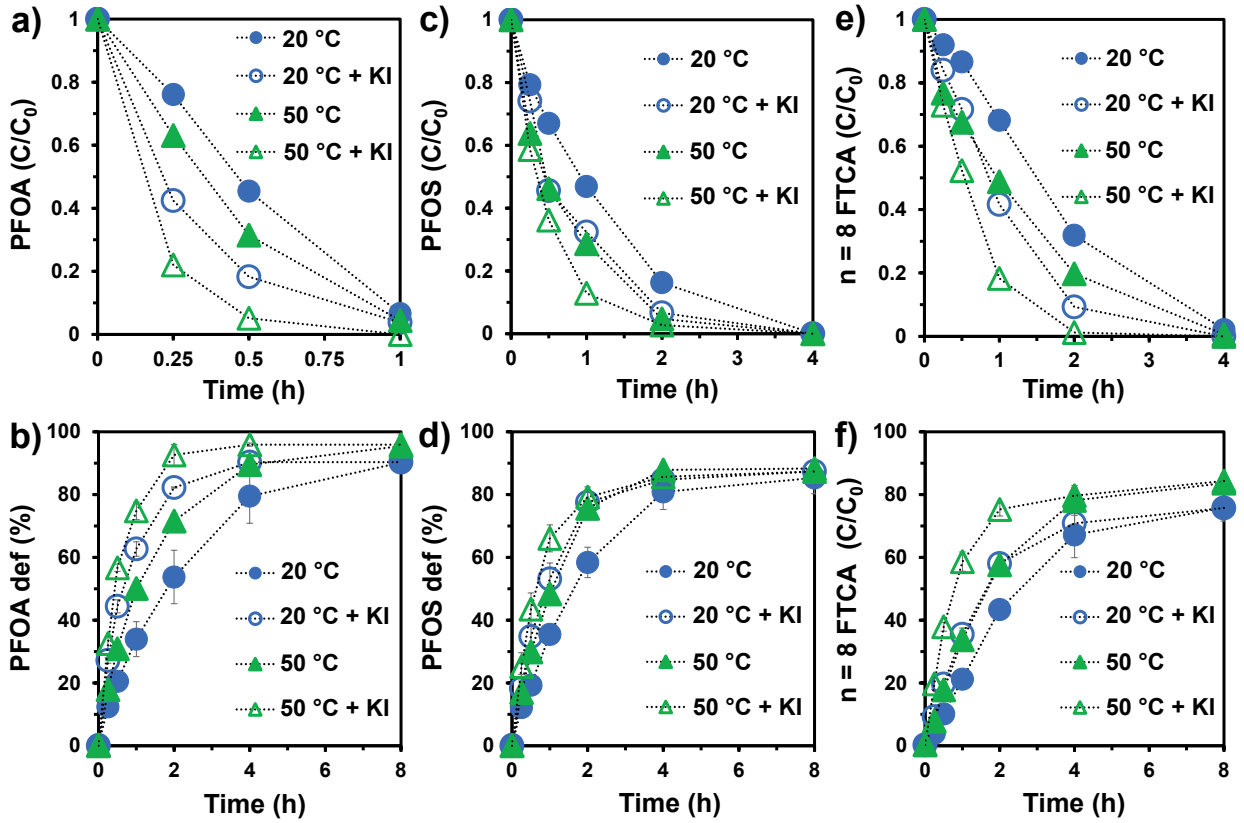

Figure ES-2. Profiles for (a, c, and e) parent compound decay and (b, d, and f) defluorination of PFOA, perfluorooctane sulfonic acid (PFOS), and n = 8 FTCA with or without KI (2 mM) at 20 °C and 50 °C.

Reaction conditions: individual PFAS (25 μM), Na_2SO_3 (10 mM), $NaHCO_3$ (5 mM), pH 12.0, and 254 nm irradiation (10 W low-pressure Hg lamp for 2 L solution).

Thermal-enhanced alkaline defluorination. The **second highlight of this project** is the systematic understanding of the structure-reactivity relationship and mechanisms for non-photochemical, non-redox defluorination of PFAS at elevated temperature and alkaline conditions. The project team found a series of H-containing PFAS allowed non-redox defluorination under alkaline conditions (pH≥9, Figure ES-3). The 6:2 FTCA ($C_6F_{13}C\mathbf{H_2}COO^-$) showed limited defluorination at pH 9.0 and 20°C, primarily via HF elimination (i.e., yielding $C_5F_{11}-CF=C\mathbf{H}-COO^-$). Elevated temperature (up to 90°C) and pH (up to 14) not only accelerated the reaction rate but also intensified the level of defluorination via additional mechanisms, many of which remained elusive. For example, $C_6F_{13}C\mathbf{H_2}COO^-$ could be further transformed into multiple PFCAs $C_nF_{2n+1}-COOH$ (n=4, 3, 2) as the end products.

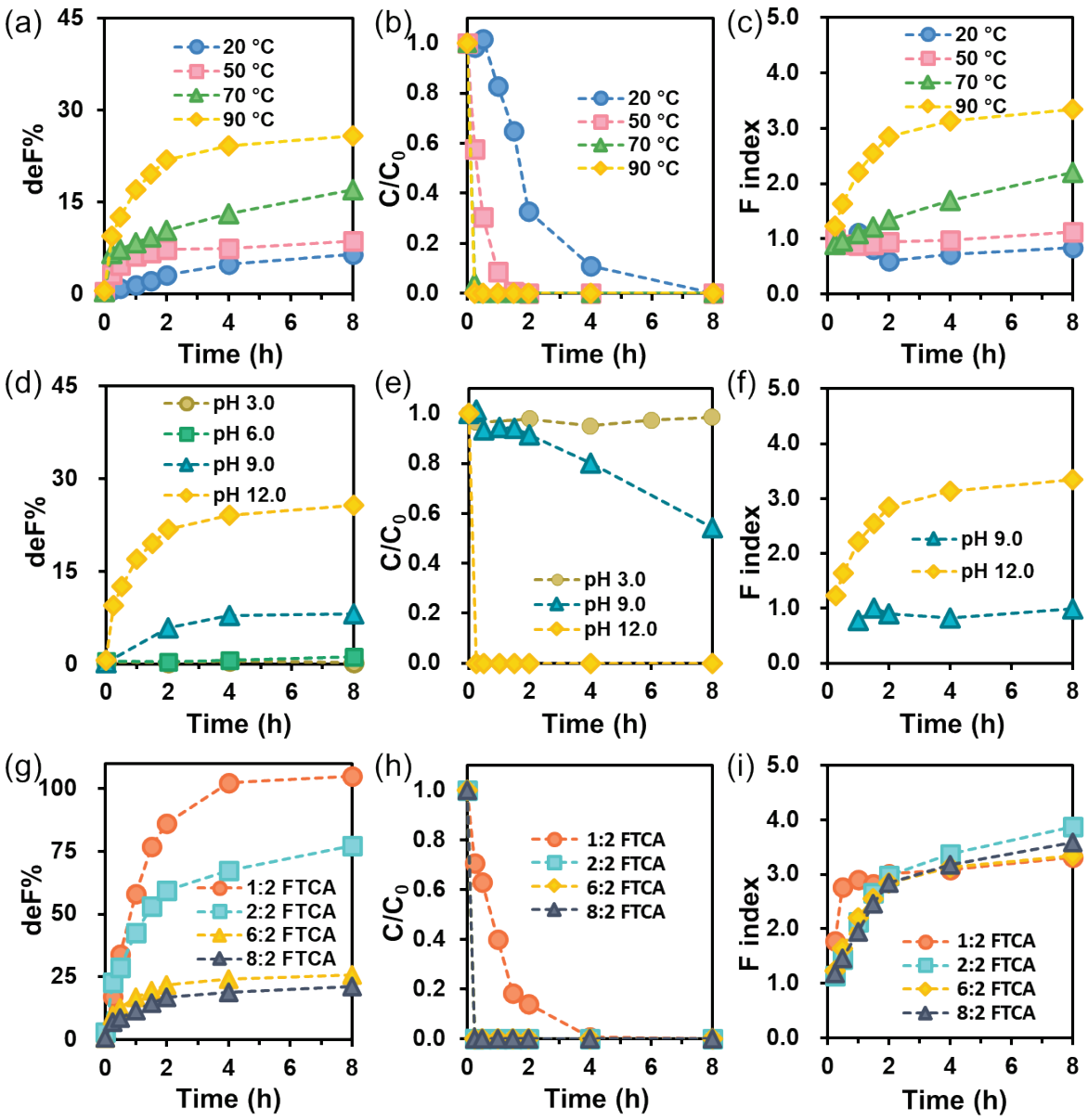

Figure ES-3. (a-c) Influence of Temperature on the Defluorination of 6:2 FTCA at pH 12.0; (d-f) Influence of pH on the Defluorination of 6:2 FTCA at pH 12.0; (g-i) Defluorination of Various n:2 FTCA (n=1, 2, 6, or 8) at pH 12.0 and 90 oC; [n:2 FTCA] = 25 µM.

The project team further extended the PFAS collection to 30+ H-containing PFAS structures (Table ES-2) and confirmed the general trend that C−H bonds with a high acidity were prone to be eliminated alongside neighboring F atoms. The resulting double bonds containing F atoms could be further defluorinated by OH^- attacks. Because of the structure specificity, heating the water at pH 12 after UV/sulfite treatment could not replace oxidation treatment to achieve 100% defluorination for a majority of PFAS. However, the findings provided important insights into the additional PFAS degradation mechanism under heated alkaline conditions (e.g., UV/sulfite at pH 12 without temperature control) and cautioned the analytical researchers on sample preservation to avoid gradual defluorination in alkaline solutions.

Table ES-2. Defluorination Performance of Various Polyfluoroalkyl Substances. [a]

entry	PFAS structure	deF% [a] [# of C-F bonds broken per molecule]	Parent compound decay rate (h^{-1})	deF% (10 M NaOH, 90°C, 2 d)
Influence of chain length of n:2 FTCA				
1	1:2 FTCA	103.5±2.12% [3.19±0.15/3F]	1.21±0.06	-
2	2:2 FTCA	83.1±8.06% (4.13±0.38/5F)	depleted in 15 min (> 11.96 h^{-1})	-
3	6:2 FTCA	25.75% [3.35/13F]	depleted in 15 min (> 11.96 h^{-1})	-
4		17.00% (@ 70 °C) [2.21/13F]	12.61	14.6%
5		8.61% (@ 50 °C) [1.12/13F]	3.18±0.32	-
6		7.67% (@ 20 °C) [0.844/13F]	1.77±0.58	-
7	8:2 FTCA	21.1% [3.59/17F]	depleted in 15 min (> 11.96 h^{-1})	-
Influence of head group of $C_nF_{2n+1}-CH_2-R$				
11	1:1 SO_3H	86.96% (2.67/3F)	1.45 ± 0.48	66.4%
10	1:1 CHO	80.04±0.49% [2.40±0.01/3F]	defluorination finished in 15 min (v > 11.96)	79.7%
8	1:1 OH	0.14±0.07%	n/d	
9	6:1 OH	0.09±0.08%	n/d	1.2%
12	3:1 NH_2	0.06%	n/d	
13	4:1 NH_2	0.06%	n/d	9.8%
14	7:1 NH_2	0.04%	n/d	4.6%
Influence of C-H bond location				
15	$CF_3CFHCOOH$	8 h 16.20% [3.82/4F]	0.04±0.01	50.6%
16	$HOOC-CF_2-CH_2-COOH$	38.91±0.31% [1.92±0.63/2F]	0.07±0.01	84.5%
17	$HC_6F_{12}COOH$	0%	-	12.0%
18	$CF_3CHFCF_2CH_2OH$	22.15±2.8% [1.32±0.17/6F]	n/d	-
19	$(CF_3)_2CHCH_2COOH$	109% [6.54/6F]	0.27±0.04	91.4%
20	$CH_3CH_2CF_2-COOH$	0.42%	-	1.1%
21	CF_3CF_2COOH	0	-	-
22	$CH_3CHFCOOH$	0.21%	-	-
23	HCF_2COOH	0%	-	82.1%
24	6:2 COOH	0%	-	0.1%
25	6:2 SO_3H	0%	-	0.6%
Influence double bond				
26	$CF_3-CH=CH-CH_2-OH$	0.50%	n/d	-
27	$CF_3-CH=CH-COOH$	12 h 1.57±0.05%	−0.01±0.00	-
28	$C_3F_7-CH=CH-COOH$	0.07±0.03%	0.01±0.00	20.3%
29	$CF_3-CF_2-CF=CF-COOH$	35.71% @ 12 h [6.44±2.2/7F]	0.10±0.03	21.6%
30	$C_5F_{11}-CF=CH-COOH$	19.75% [2.37/12F]	1.75±0.58	-
32	$CF_2=CF-CH_2-CH_2-COOH$	3.89% @ 12 h [0.58/3F]	0.03±0.051	-

[a]Unless specified otherwise, the reaction conditions are pH 12.0 and 90°C and the deF% were obtained at the end of the reaction.

Further optimization of energy efficiency. The **third highlight of this project** was the proof-of-concept that the UV lamp could be used as the main source of heat to achieve enhanced defluorination in both reaction rate and depth of destruction. The results reflected the overall effect of thermal energy generation and UV irradiation by low-pressure UV lamps on PFAS degradation. With the 2 L reactors used in this study, two 10 W UV lamps provided the most cost-effective treatment of both PFOA and PFBS (Figure ES-4).

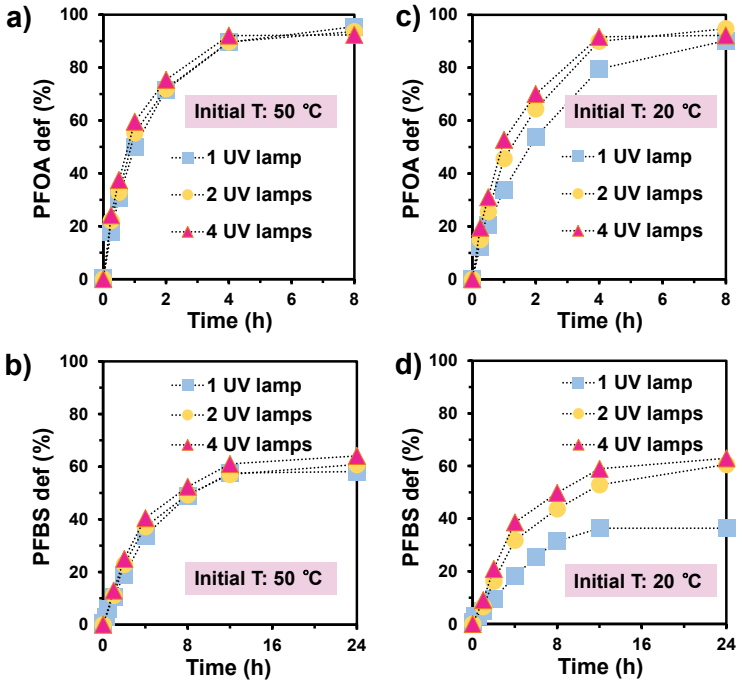

Figure ES-4. Time profiles for PFOA and PFBS defluorination at the initial temperature of (a and b) 50 °C and (c and d) 20 °C.

Reaction conditions: individual PFAS (25 μM), Na_2SO_3 (10 mM), $NaHCO_3$ (5 mM), pH 12.0, and 254 nm irradiation (10 W low-pressure Hg lamps for 2 L solution). No cooling water was used.

The thermal energy from UV lamps was sufficient to bring the water temperature to the optimal 50°C (Table ES-3), which allowed deeper defluorination of the recalcitrant PFBS. Preheating the water to the optimal temperature was not necessary if considering the electrical energy consumption (Table ES-4). Overall, the heat dissipated from the UV lamps provided significant enhancement in the rate and extent of PFAS defluorination.

Table ES-3. Water Heating by UV Lamps.[a]

Number of UV lamps	Temperature of water (2 L)			
	Start @ 20 °C		Start @ 50 °C	
	@ 4h	@ 8h	@ 4h	@ 8h
1	36 °C	36 °C	50 °C	50 °C
2	48 °C	53 °C	53 °C	53 °C
4	65 °C	73 °C	73 °C	73 °C

[a]When one 10 W UV lamp was used, a heating plate was needed to achieve the water temperature at 50°C. With two and four UV lamps, a heating plate was not used after the lamps were turned on.

Table ES-4. Energy Consumption to Achieve Maximum PFAS Defluorination with Varying Numbers of UV Lamps.[a]

Number of UV lamps	Energy consumption to achieve maximum defluorination (kJ for 2 L and kWh/m^3)			
	Start @ 20 °C[b]		Start @ 50 °C[c]	
	PFOA	PFBS	PFOA	PFBS
1	144 (20)	432 (60)	390 (54.2)[d]	678 (94.2)[d]
2	288 (40)	864 (120)	534 (74.2)	1110 (154.2)
4	576 (80)	1728 (240)	822(114.2)	1974 (274.2)

[a]Reaction conditions: PFAS (25 μM), Na_2SO_3 (10 mM), $NaHCO_3$ (5 mM), pH 12.0, and 254 nm irradiation (10 W low-pressure Hg lamp for 2 L solution).
[b]The energy consumption is calculated as n×t×36, where n represents the number of UV lamps, t denotes the time required to reach maximum defluorination (h), and 36 represents the energy consumption per hour by a 10 W UV lamp (kJ).
[c]The energy consumption is calculated as 245.5+n×t×36, where 245.5 represents the energy consumption for heating 2 L of water from 20°C to 50 °C (kJ).
[d]Estimating the energy consumption required to maintain the temperature at 50°C is not straightforward and not included here. This value could greatly vary by thermal insulation settings, which was not studied by this project except for aluminum foil wrapping outside the reactor.

Key Information for Site Managers

1. Elevating the temperature facilitates e_{aq}^- in cleaving the C–F bonds but decreases the quantum yield of e_{aq}^-. Consequently, the overall deF% reached the maximum at 50 °C, where the positive effect outweighed the negative effects to the greatest extent. In practical applications, it is essential to consider the energy consumed in raising the temperature to 50 °C. In the study involving 2 L water and a 10 W light source, the thermal energy needed to heat the water from 20 to 50 °C (without heat dissipation) is comparable to the electrical energy for the UV lamp working over 6.8 h (see main text for details). Hence, it is not advisable to raise the temperature to 50 °C for wastewater mainly containing PFAS structures that are easily degradable, such as PFCAs, PFOS, and n=8 FTCA.
2. The final decay% and deF% enhancement at 50 °C is particularly substantial for short-chain PFSAs and FTCAs, which possess relatively strong C–F bonds. In such scenarios, elevating the temperature could be beneficial for wastewaters primarily containing those types of PFAS. Even without using dedicated equipment to heat the water to 50 °C, PFAS defluorination can be enhanced by the rise in temperature by the UV lamps. For example, the 10 W UV lamp raised the temperature of 2 L water from 20 to 36°C within 4 h (without insulation). The deF% of n=6 FTCA and perfluorohexane sulfonic acid (PFHxS) in this study (slowly heated from 20 to 36°C) were 26.7% and 17.9% higher, respectively, compared to the systems where temperature was maintained at 20 °C.
3. In cases where the reaction temperature is elevated excessively (e.g., > 90 °C if a high-power medium/high-pressure Hg lamp is used or multiple low-pressure Hg lamps are used), a cooling operation may be needed to facilitate the optimal PFAS defluorination.

4. The overlooked heat from UV lamps could greatly aid in PFAS defluorination. For the 2 L reactor used in this study, two 10 W UV lamps proved to be the most efficient configuration. For larger reactor designs, temperature control is very important to ensure the water temperature is within the range for optimal defluorination performance. The cooling water setting for academic research (toward a good temperature control at the commonly adopted 20°C across literature) should not be used for practical applications. Instead, thermal insulation should be applied to the reactor parts to preserve the unavoidable heat from UV lamps. In addition, extra heating equipment might be necessary, depending on the number of UV lamps to be used. The detailed parameters need to be determined when pilot- or full-scale reactors are built.
5. The strong electronegativity of the F atom increases the acidity of the H atom in the polyfluoroalkyl structures, making it prone to attack by aqueous OH^-, allowing HF elimination and further transformations. Besides, the F atom on double bonds is also subject to defluorination under alkaline conditions. These findings provide deeper insights into PFAS transformation in both natural and engineering systems. It is important to consider that H-containing PFAS released into the environment or generated from the transformation of other PFAS may undergo spontaneous defluorination.
6. It is highly worth noting that PFAS stock solutions and reaction samples of H-containing PFAS might be unstable under alkaline conditions. For such chemicals (the project team has provided a large variety of examples in this project), the common practice of using excess NaOH to help dissolve/stabilize acid-type PFAS should be used with caution.

5.0 IMPLICATIONS FOR FUTURE RESEARCH AND BENEFITS

The findings have answered most research questions proposed for this limited-scope project. It has confirmed the positive effect of thermal energy, which is the dominant way of electrical energy dissipation from UV lamps (i.e., all energy not utilized for chemical reaction will eventually transform into heat). The findings have been provided to the ESTCP project (ER21-5152) on the treatment of still bottom brines and foam fractionation concentrates and other real PFAS-containing hazardous material treatment cases.

Because of the structure specificity, heating the water at pH 12 after UV/sulfite treatment could not replace oxidation treatment to achieve 100% defluorination for a majority of PFAS. However, the findings provided important insights into the additional PFAS degradation mechanism under heated alkaline conditions (e.g., UV/sulfite at pH 12 without temperature control) and cautioned the analytical researchers on sample preservation to avoid gradual defluorination in alkaline solutions. Detailed mechanisms, particularly how the hydroxide attack on the double bond could trigger deeper degradation and eventually form PFCAs in various lengths, remained elusive. Further understanding of such mechanism could be of high value to (1) develop new PFAS degradation technologies using low-cost chemicals and (2) achieve a deeper understanding of PFAS transformation in natural and engineered photochemical systems and microbial systems. Particularly, whether a defluorination step requires the participation of photochemical/biological species (e.g., radicals/enzymes) or simply an alkaline media.

This study did not further test the better-insulated reactors (e.g., using plastic foams or glass wools outside the container rather than aluminum foil) because the pilot- and full-scale systems will have more comprehensive considerations and design guidelines on the heat transfer aspects, such as (1) what part(s) of the system (e.g., reservoir, pipes, and UV module) can be insulated and (2) whether controlled heating and cooling modules are still required from the engineering perspectives. Thus, in this study, the project team primarily focused on the temperature values and the proof-of-concept rather than developing detailed approaches for heat transfer control.